Diffraction and spectral statistics in systems with a multilevel scatterer

A. Matzkin

Laboratoire de Spectrométrie Physique (CNRS Unité 5588), Université Joseph-Fourier Grenoble-I, Boîte Postale 87,
F-38402 Saint-Martin, France

T. S. Monteiro

Department of Physics and Astronomy, University College London, Gower Street, London WC1E 6BT, Great Britain

A semiclassical framework to interpret the spectral rigidity of a system containing a scatterer with internal states is developed. Our prototype system is a scaled Rydberg molecule in an external magnetic field, where the core is a multilevel scatterer: the potential sheet in which the outer electron moves depends on the quantum state of the core. Thus the electron-core collision, interpreted in terms of the diffraction of the semiclassical waves associated with the outer electron on the core, can result in a change of the electron's dynamical regime. We examine the contribution of the diffraction to the spectral rigidity by obtaining the diffractive Green's function in the semiclassical limit. We concurrently determine this contribution from accurate quantum spectra and compare numerically the semiclassical and quantum results. Our findings indicate that, in a system with a multilevel scatterer, the diffractive contribution to the spectral rigidity cannot be accounted for by a simple universal expression, but rather depends on system specific nonuniversal terms: the quantum properties of the scatterer (reflected by the relative values of the phase shifts in the different channels) and the classical properties of the shortest periodic orbits in the different dynamical regimes.

I. INTRODUCTION

A fundamental property of quantum systems concerns the statistical distributions of the energy levels. On the one hand, it is well known that regular quantum systems are characterized by level clustering, whereas irregular systems display level repulsion. On the other hand, there is ample evidence that the spectral fluctuations of the energy levels depend on the nature of the corresponding classical system. The main tool employed in connecting both approaches is the semiclassical trace formula, giving the modulations in the quantum density of states in terms of classical periodic orbits. Since for generic systems semiclassics does not resolve individual states, such methods fail for short-range statistics (relative to the mean level spacing), such as the nearest-neighbor distribution, but should give appropriate results for longer-range correlations. Indeed, in a seminal work, Berry [1] showed how long-range level correlations could be obtained in terms of periodic orbits. In particular, the spectral rigidity $\Delta(L)$, linked to the two-point correlation function (and to its Fourier transform, the spectral form factor), was shown to depend on mean properties of the long-time classical dynamics (giving rise to universal behavior) and on the short periodic orbits (which give rise to a system-dependent behavior).

When a scatterer is added to the system, the potential acquires discontinuities. In the semiclassical limit, this gives rise to additional terms in the trace formula which have their origin in the diffraction of the waves on the scatterer [2]. The orbits that hit the scatterer are termed "diffractive," as opposed to the "geometric" ones that exist in the scatter-free system. Although the additional terms in the trace formula have a higher $\hbar$ dependence, it is known that they can still

have an influence in the spectral statistics as $\hbar \rightarrow 0$. For example, Sieber has given the correction to the spectral form factor for simple systems displaying geometry-dependent diffraction [3]; it was also shown that, by including correlations between diffractive and geometric orbits, the form factor of a system with a pointlike scatterer was left unchanged in the chaotic regime [4,5]; more recently, the effect of localized perturbations in billiards was investigated [6,7].

In this work, we investigate the spectral rigidity for a system presenting a multilevel quantum scatterer. This means the scatterer behaves as a quantum object (as opposed to the geometry-dependent scattering case considered up to now) which may exchange energy with the semiclassical waves. Our prototype system studied here will be a Rydberg molecule in an external field; the excited electron will be treated semiclassically when it roams far from the residual molecular core, but the scattering process between the core and the electron is treated quantum mechanically. The main feature is that scattering may lead to a change in the internal quantum state of the core, in which case the outer electron moves in different potential sheets prior to and after the collision. Although long-range correlations for the hydrogen atom in a magnetic field were studied quite early [8], very little has been done for nonhydrogenic atoms: numerical results for lithium were presented in Ref. [9] along with a phenomenological formula to take into account the diffractive effects. Fluctuation properties for Rydberg molecules in field-free space were studied by Lombardi and Seligman [10]; however, scattering was not treated as a diffractive process but by means of a classical model that turns out to be valid only for very high rotational quantum numbers.

We will determine below the diffractive contribution to the spectral rigidity, by undertaking exact quantum calculations on the one hand and by deriving the semiclassical for-

malism which takes the diffractive orbits appropriately into account. In Sec. II a brief presentation of the model is given. In Sec. III the diffractive Green's function is constructed with the aim of obtaining the additional terms entering the trace formula. This allows us to determine the diffractive contribution to the spectral rigidity (Sec. IV) by employing a semiclassical approach. Our formulas account both for non-universal terms (due to individual short-period orbits) and universal terms (generated by longer orbits). We then compare in Sec. V the rigidity obtained from the quantum calculation of the energy levels to the predictions of the semiclassical model; by changing the properties (quantum phase shifts) of the scatterer we contrast various situations. We examine in particular the effects of elastic and inelastic collisions on the energy level correlations. We then discuss the results and the relevance of the approximations made, and conclude.

II. DESCRIPTION OF THE MODEL

A. Scaled electron dynamics in a Coulomb and magnetic field

The hydrogen atom in an external magnetic field is a well-known paradigm of quantum chaos [11]. The classical dynamics of the electron does not depend independently on its energy E and the magnetic field strength γ but is invariant (up to a scale factor) provided $\epsilon = E\gamma^{-2/3}$ is constant. ϵ is the scaled energy and the dynamics goes from the near-integrable ($\epsilon \lesssim -0.8$) to the chaotic ($\epsilon \lesssim -0.1$) regime. Using scaled variables $(\tilde{r} = \gamma^{2/3}r, \tilde{p} = \gamma^{-1/3}p)$ in the Schrödinger equation leads to a generalized eigenvalue problem where $\hbar$ is replaced by $\gamma^{1/3} \equiv \hbar_{eff}$, which plays the role of an effective Planck constant. Therefore, the scaling property allows us to study the semiclassical limit of the quantum problem while keeping the classical dynamics constant.

This scaling property still holds for simple nonhydrogenic Rydberg atoms (e.g., [12]). The outer electron senses only the Coulomb and magnetic fields (exactly as in hydrogen) except in a small zone around the core (the inner region). But to a good approximation the core–Rydberg-electron interaction is energy independent, so that in practice the scaling properties hold.

B. The model: A scaled molecule

However, for generic atoms and even for the simplest diatomic molecule, the outer electron may exchange energy with the core, and the quantum state of the core may also change. Therefore, in the outer zone the Rydberg electron senses only the Coulomb and magnetic fields, but following the collision with the core the energy will change if the energy partition between the outer electron and the core is modified. In the scaled problem, this involves a change in the scaled energy ϵ of the electron; the collision therefore modifies the dynamical regime. However, the core–Rydberg-electron interaction in the inner zone cannot be scaled, since this interaction depends on physical properties of the core that are independent of the outer electron's energy or magnetic field strength.

The model employed in this work to investigate the spectral statistics is that of a scaled diatomic molecule. This model was described in detail in Refs. [13,14], in which we studied the photoabsorption spectrum (the density of states weighted by dipole transition elements) for a molecule such as H_2; we compared the quantum results with a semiclassical formalism based on closed orbit theory. Here we will use the same quantum code to obtain the levels for the scaled molecule in a magnetic field.

In our scaled molecule model, the molecule is partitioned into an outer electron and the residual ionic core. The core can be in one of four quantum states: the ground state has the quantum numbers $N=0$, $M_N=M$; physically, N is the rotational quantum number of the core, M_N is the projection of N on the field axis, and M is the projection of the total angular momentum J of the molecule on the field axis. There are three excited core states; they have the same rotational number $N=2$, but different projections $M_N=M-1$, M, $M+1$. The three excited states are degenerate in energy (which physically amounts to neglecting the linear Zeeman effect). M is the only conserved quantum number (in what follows we will set $M=0$). The energy partition leads to the following relationship between the scaled energies ϵ_N of the outer electron associated with different core states N:

$$\epsilon_{N=0} = \epsilon_{N=2} + 2(2+1)\tilde{B}_r. \tag{2.1}$$

$\tilde{B}_r$ is the scaled rotational constant, which is obtained by artificially scaling the real molecular rotational constant (see Sec. III F of [14]). In the present work, $\tilde{B}_r$ may be seen as a parameter that sets the scaled energy gap between the two dynamical regimes. Note that for $N=2$ the dynamical regime for the outer electron does not depend on the value of M_N, but the potential sheet in which the electron moves does depend on whether $M_N=0$ or $|M_N|=1$.

C. The T matrix

We briefly describe the scattering process between the outer electron and the core. Far from the core, the electron is affected by the core in one of its alternative core states $|j\rangle \equiv |N_j M_{N_j}\rangle$ and senses only (in addition to the external magnetic field) the long-range Coulomb field due to the positive ionic core; the orbital momentum of the outer electron l is coupled to the magnetic field axis, and m is its projection (we have $M=M_{N_j}+m_j$). However, in the comparatively very small region near the core, the external field is negligible and the electron is strongly coupled to the molecular core: the global molecule is then described in the Born-Oppenheimer frame $|\alpha\rangle \equiv |\Lambda_\alpha J_\alpha l_\alpha\rangle$. Λ is the projection of the electronic angular momentum on the molecular axis, on which l is now quantized. The descriptions in the two regions are linked by a unitary frame transformation, with elements $\langle j|\alpha\rangle^M$ that are easily determined [15]. The upshot is that the short-range interaction between the core and the outer electron is best described in the $|\alpha\rangle$ basis, where the $\mathfrak{T}$ matrix is diagonal, with elements

$$\mathfrak{T}_\alpha = \frac{1 - e^{2i\pi\mu_\alpha}}{2i}. \tag{2.2}$$

$\pi\mu_\alpha$ is the phase shift induced by the short-range interaction of the core when the outer electron is described in the $|\alpha\rangle$ basis.

The T matrix, which gives the transition probabilities between states of the outer region, described in the $|j\rangle$ basis, contains the scattering information that will be of interest for the diffraction process. It is obtained from the $\mathfrak{T}$ matrix by implementing the frame transformation (e.g., [14])

$$T_{jj'} = \sum_\alpha \langle j|\alpha\rangle \mathfrak{T}_\alpha \langle \alpha|j'\rangle, \tag{2.3}$$

where we have dropped the M dependence on the frame transformation and on the resulting T matrix. Thus the T matrix depends on the electronic quantum defects μ_α, which give the phase shifts induced by the short-range core-electron interaction in the $|\alpha\rangle$ basis. In our model, we assume there are only two independent quantum defects: μ_Σ for the state $|\Lambda = 0, J=1, l=1\rangle$ and μ_Π for the states $||\Lambda|=1, J=1, l=1\rangle$. From the physical standpoint, this corresponds to investigating the statistics of states excited from the ground state $|\Lambda = 0, J=0, l=0\rangle$ of the molecule, assuming that the outer electron does not penetrate into the core when $l \geq 2$.

To sum up, the characteristics of the diffractive scatterer depend on the two quantities μ_Σ and μ_Π, which in turn determine the T-matrix elements between states $|j\rangle$ and $|j'\rangle$ where $|j\rangle$ and $|j'\rangle$ stand for the four core states $|N=0, M_N =0\rangle$, $|N=2, M_N=0\rangle$, $|N=2, M_N=\pm 1\rangle$.

III. THE DIFFRACTIVE GREEN'S FUNCTION

A. General remarks

The geometrical theory of diffraction for electromagnetic waves in the short-wavelength limit is well established [16]. The use of analogous techniques in semiclassical physics is more recent (e.g., [2,17,18]). The aim is to extend periodic orbit theory in the cases where the semiclassical waves, carried by classical trajectories, encounter discontinuities of the order of their de Broglie wavelengths. This diffractive process is incorporated into periodic orbit theory by determining the diffractive part of the Green's function. Indeed, in the absence of the diffractive scatterer, quantum properties of the system are obtained from the (scatterer-)"free" Green's function $G_0(E)$ in terms of the periodic orbits of the "free" system, which are usually termed geometric periodic orbits. When the scatterer is added, the total Green's function is

$$G(E) = G_0(E) + G_D(E), \tag{3.1}$$

where G_D is the diffractive Green's function to be obtained in terms of the periodic orbits (PO's) that hit the scatterer. These "diffractive PO's" produce additional fluctuations in the energy spectrum.

In the present section we will determine the diffractive Green's function for our system—a scaled molecule for which the scatterer (the molecular core) presents many internal states. In the limit in which the scatterer has only one

quantum state, this gives the diffractive Green's function for simple nonhydrogenic atoms, which have been intensively investigated and for which a phenomenological global diffractive contribution was obtained [19]. Our approach will heavily rely on known results obtained from closed orbit theory [20], a version of PO theory that has been employed to investigate the photoabsorption spectrum of Rydberg atoms and molecules in external fields. However, unlike Gutzwiller's approach [21], which is based on a semiclassical approximation to the propagator written in terms of a path integral, closed orbit theory relies on the semiclassical approach due to Maslov [22], grounded on a semiclassical approximation to the transport and phase equations. In what follows, we will use a straightforward identification between both approaches; an elegant and rigorous treatment connecting both approaches was given by Littlejohn [23].

B. Determination of the diffractive Green's function

1. Two-dimensional semiclassical "free" Green's function

In the outer region, the excited electron is subjected to the Coulomb and magnetic fields, yielding a three-dimensional axially symmetric system; the axis of symmetry is along the z axis, chosen in the direction of the magnetic field. We can therefore separate the azimuthal degree of freedom (with quantum number m, the projection of l on the z axis, and azimuthal angle φ) and write the "free" Green's function in the semiclassical limit as

$$G_0(E) = \sum_m |m\rangle\langle m|G_{sc}^{(m)}(\mathbf{r}',\mathbf{r},E), \tag{3.2}$$

where $G_{sc}^{(m)}$ is the symmetry reduced semiclassical Green's function corresponding to the azimuthal number m [since the effective two-dimensional (2D) potential depends on m]. It is straightforward to show [24] that $G_{sc}^{(m)}$ is the usual two-dimensional semiclassical Green's function describing propagation from $\mathbf{r}$ to $\mathbf{r}'$, which are two points in the 2D axial plane. G_{sc} is given by [25]

$$G_{sc}(\mathbf{r}',\mathbf{r},E) = \sum_k (\hbar\sqrt{2\pi\hbar})^{-1}|\mathcal{D}_k|^{1/2}$$
$$\times \exp i[S_k(\mathbf{r}',\mathbf{r}) - \mu_k\pi/2 - 3\pi/4]. \tag{3.3}$$

S_k and μ_k are the action and the Maslov index for the kth trajectory connecting $\mathbf{r}$ and $\mathbf{r}'$. $\mathcal{D}_k$ is the Jacobian determinant giving the density of paths; in a local coordinate system $\mathbf{r}=(q,q^\perp)$, where $q(q^\perp)$ lies along (perpendicular to) the trajectory and $p(p^\perp)$ is the conjugate momentum, we have

$$\mathcal{D}_k = \frac{1}{\dot{q}\dot{q}'}\left(\frac{\partial p_k'^\perp}{\partial q^\perp}\right)_{q'^\perp}. \tag{3.4}$$

Equation (3.2) gives the Green's function for the hydrogen atom in a magnetic field. Anticipating the multiple-core-state case, we can write the Green's function for a set of hydrogen atoms at different energies E_j as

$$G_0(E) = \sum_j |jm_j\rangle\langle jm_j| G_{sc}^j(\mathbf{r}',\mathbf{r},E_j). \qquad (3.5)$$

With $|j\rangle = |N_j M_{N_j}\rangle$ and $E = E_j^+ + E_j$, Eq. (3.5) gives the Green's function for a sum of independent systems each comprised of an outer electron at energy E_j associated with a molecular core at energy E_j^+ which interacts with its outer electron only through the long-range Coulomb field. This is the "free" Green's function in the outer region for our model.

2. Green's function in the inner region

In the inner region, near the core, the external magnetic field can be neglected and the system displays the spherical symmetry of the Coulomb field with coordinates $\mathbf{r} = (r, \theta)$ (the anisotropy created by the core-electron interaction is embodied in the quantum defects, which appear as radial phase shifts). The quantum mechanical "free" Green's function takes into account only the Coulomb interaction:

$$G_0(r_2, r_1, E) = -16\pi \sum_j |jm_j\rangle$$

$$\times \langle jm_j| f_{l_j}(r_1) Y_{l_j m_j}^*(\theta_1) g_{l_j}^+(r_2) Y_{l_j m_{j'}}(\theta_2), \qquad (3.6)$$

where $r_2 > r_1$ and $Y_{l_j m_j}(\theta_i)$ stands for the spherical harmonic $Y_{l_j m_j}(\theta_i, 0)$. f_l and g_l are standing Coulomb waves, respectively regular and irregular at the origin, and $g_l^\pm = (g_l \pm i f_l)$ are outgoing and incoming Coulomb waves.

If we now take into account the short-range interactions, the total Green's function is given in the inner zone by projecting the resolvent equation $G = G_0 + G_0 T G_0$, yielding [26]

$$G(r_2, r_1) = -16\pi \sum_j |jm_j\rangle g_{l_j}^+(r_2) Y_{l_j m_j}(\theta_2) \Bigg\{ \sum_{j'} [\delta_{jj'} f_{l_{j'}}(r_1)$$

$$+ T_{jj'} g_{l_{j'}}^+(r_1)] Y_{l_{j'} m_{j'}}^*(\theta_1) \langle j'm_{j'}| \Bigg\}. \qquad (3.7)$$

Note that the label m_j in $|jm_j\rangle$ is redundant, since $M = M_j + m_j$ is fixed; we shall therefore subsume m_j under the label j. Of course, Eqs. (3.6) and (3.7) can also be written in the $|\alpha\rangle$ basis. A solution $|\psi_j\rangle$ of the full Hamiltonian in the inner zone is related to a standing-wave solution $|\xi_j\rangle = f_{l_j}(r) Y_{l_j m_j}(\theta)|j\rangle$ of the scatterer-free Hamiltonian via the Lippman-Schwinger equation

$$|\psi_j\rangle = |\xi_j\rangle + G_0 T |\xi_j\rangle. \qquad (3.8)$$

3. Connecting the inner and outer zones

Equations (3.5) and (3.7) cannot be connected directly, since the relevant Green's functions obey different boundary conditions. We will rely instead on closed orbit theory techniques and consider the following physical situation (Fig. 1). Let the core be in state j and $\mathbf{r}_1$ and $\mathbf{r}_2$ two points in the outer region. We want to find the waves arriving at $\mathbf{r}_2$ produced by a unit source placed at $\mathbf{r}_1$. Semiclassically, there are three types of waves carried by three different types of trajectories. The direct propagation from $\mathbf{r}_1$ to $\mathbf{r}_2$, obviously without af-
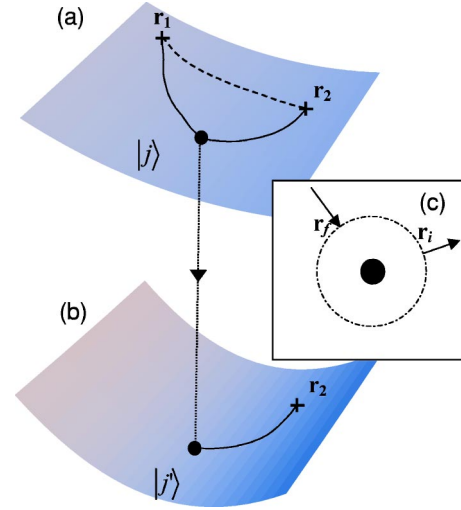
FIG. 1. (a) shows the potential sheet associated with the core scatterer in state $|j\rangle$ and (b) shows another potential sheet lying lower in energy associated with the scatterer in state $|j'\rangle$. A unit source placed at $\mathbf{r}_1$ reaches $\mathbf{r}_2$ either by direct propagation [dashed line in (a)], by hitting the core while staying on the same potential sheet [solid line in (a), elastic scattering], or by changing to another potential sheet after the collision with the core [solid line from $\mathbf{r}_1$ to the core in (a) and from the core to $\mathbf{r}_2$ in (b), inelastic scattering]. (c) shows schematically the matching between the semiclassical waves outside the boundary circle and the quantum mechanical wave function in the inner zone (see text).

fecting the state of the scatterer [dotted line in Fig. 1(a)] is due to the "free" Green's function; this is the standard situation which will not concern us in this paper. The *elastic* diffractive trajectory [solid line in Fig. 1(a)] links $\mathbf{r}_1$ to $\mathbf{r}_2$ via a hit at the core, without changing the state of the core. The trajectory arrives near the scatterer at some point $\mathbf{r}_f = (r_0, \theta_f)$ and leaves the core region passing through $\mathbf{r}_i = (r_0, \theta_i)$ [see Fig. 1(c)]. r_0 is the radius of a boundary circle within the inner region but for which the approximations made in the outer region still hold [14,20]. The third type of trajectory is the *inelastic* diffractive one [Figs. 1(a) and 1(b)]: the electron arrives on the core in state j [Fig. 1(a)] but leaves the inner region with the core in state j' [Fig. 1(b)]. Usually inelastic scattering is accompanied by a change in the potential sheet in which the electron moves.

To find the Green's function in the inner zone, we proceed as in closed orbit theory (e.g., Sec. III D of [14]), except that here the initial wave is a unit source placed at $\mathbf{r}_1$. On the boundary circle, the incoming wave is $G_{sc}^j(\mathbf{r}_f, \mathbf{r}_1, E_j)|j\rangle$ with G_{sc} given by Eq. (3.3). On the other hand, in the inner region the most general solution is given by the sum $\sum_{j'} c_{j'}|\psi_{j'}\rangle$ where the $|\psi_{j'}\rangle$'s are given by Eq. (3.8); the expansion yields

$$\sum_{j'} |j'\rangle Y_{l_{j'} m_{j'}}(\theta) \sum_j c_j [\delta_{jj'} f_{l_{j'}}(r) + T_{jj'} g_{l_{j'}}^+(r)]. \qquad (3.9)$$

The coefficients c_j are now determined by matching the incoming part of this expression to the incoming semiclassical wave function. This match is done in the stationary phase approximation (for each incoming trajectory k, the integral

on θ_f is performed along the angle of stationary phase θ_{fk}). This gives

$$c_j = \hbar^{1/2} e^{-l_j \pi} e^{-i\pi/2} 2^{9/2} \pi^2 r_0^{1/2} e^{i\sqrt{8r_0}}$$

$$\times \sum_k \sin \theta_{f_k} Y_{l_j m_j}^*(\theta_{f'k}) G_{sc(k)}^j(r_0, \theta_{fk}; \mathbf{r}_1, E_j), \quad (3.10)$$

where we have denoted by $G_{sc(k)}^j$ the kth term of the sum over the trajectories [i.e., the expression to the right of the sum symbol in Eq. (3.3)].

The outgoing wave (from the region near the core toward $\mathbf{r}_2$) is given by the core-scattered part of Eq. (3.9),

$$\psi_{\text{out}}(\mathbf{r}) = \sum_{j'} |j'\rangle Y_{l_{j'} m_{j'}}(\theta) \sum_j c_j T_{jj'} g_{l_{j'}}^+(r). \quad (3.11)$$

Beyond the boundary circle $\mathbf{r}_i = (r_0, \theta_i)$, this outgoing wave is propagated semiclassically. Applying Maslov's theory, we write the wave function in shorthand notation as

$$\psi_{\text{out}}(\mathbf{r}) = \sum_{j'} |j'\rangle \sum_q \sqrt{\rho_q^{j'}(\mathbf{r})} \exp i(S_q^{j'} - \mu_q^{j'} \pi/2 - 3\pi/4),$$

$$(3.12)$$

where the solution of the transport equation for the density ρ gives [22]

$$\rho_q^{j'}(\mathbf{r}) = \frac{J_3(t_0, \theta_{iq})}{J_3(t, \theta_{iq})} \rho_0^{j'}(\theta_{iq}). \quad (3.13)$$

$(\rho_0^{j'})^{1/2}$ is the wave function on the boundary circle (with the core in state $|j'\rangle$). J_3 is a three-dimensional Jacobian, given by $J_3(t, \theta_{iq}) = r^2 \sin \theta J(t, \theta_{iq})$, where $J(t, \theta_{iq})$ is the standard Jacobian in the 2D plane:

$$J(t, \theta_{iq}) = \det \left| \frac{\partial(r, \theta)}{\partial(t, \theta_{iq})} \right|. \quad (3.14)$$

Equations (3.13) and (3.14) describe the divergence of neighboring trajectories starting on the boundary circle at time t_0 and arriving at $\mathbf{r}$ at time t, and are thus akin to the determinant appearing in the semiclassical Green's function (see Appendix A).

Using the asymptotic expansion for $g_{l_j}^+(r_0)$ in the zero-energy approximation as in [14], we have

$$[J_3(t_0, \theta_{iq}) \rho_0^{j'}(r_0)]^{1/2} = e^{i\sqrt{8r_0}} \sum_j \mathcal{Z}_{qk}^{j'j} G_{sc(k)}^j(r_0, \theta_{fk}; \mathbf{r}_1, E_j)$$

$$(3.15)$$

with

$$\mathcal{Z}_{qk}^{j'j} = \sum_{l_{j'}} \hbar^{1/2} r_0^{1/2} 2^3 \pi^{3/2} e^{-i(l_j + l_{j'})\pi}$$

$$\times \sqrt{\sin \theta_{iq}} Y_{l_{j'} m_{j'}}(\theta_{iq}) \sin \theta_{fk} Y_{l_j m_j}^*(\theta_{fk}) T_{jj'},$$

$$(3.16)$$

where we have used Eq. (3.10). We finally use Eq. (A5) and put the outgoing wave (3.11) at $\mathbf{r}_2$ as

$$\psi_{\text{out}}(\mathbf{r}_2) = \hbar \sqrt{2\pi\hbar} \sum_{j'} |j'\rangle \sum_{q,k} \mathcal{Z}_{qk}^{j'j} e^{2i\sqrt{8r_0}} \sqrt{2r_0 \sin \theta_{iq}} G_{sc(q)}^{j'}$$

$$\times (\mathbf{r}_2, r_0, \theta_{iq}; E_{j'}) G_{sc(k)}^j(r_0, \theta_{fk}; \mathbf{r}_1, E_j). \quad (3.17)$$

4. Diffraction coefficient

The content of Eq. (3.17) is the following. A unit source is placed at $\mathbf{r}_1$ with the core being in state $|j\rangle$. These waves are carried by classical trajectories; some of these trajectories, labeled k, hit the core with an angle θ_{fk}. Those trajectories are continued in the region near the core by the quantum mechanical scattering process, which results in outgoing waves, propagating semiclassically along trajectories q, with the core now being in a state $|j'\rangle$. $\psi_{\text{out}}(\mathbf{r}_2)$ gives the wave function at $\mathbf{r}_2$ resulting from the superposition of the possible states $|j'\rangle$ populated after the collision. The Green's function G_D corresponding to this diffractive process is given by summing Eq. (3.17) over the possible quantum states of the scatterer,

$$G_D(\mathbf{r}_2, \mathbf{r}_1; E) = \sum_{j,j'} \sum_{q,k} G_{sc(q)}^{j'}(\mathbf{r}_2, 0; E_{j'})$$

$$\times |j'\rangle \mathcal{C}_{qk}^{j'j} \langle j| G_{sc(k)}^j(0, \mathbf{r}_1; E_j), \quad (3.18)$$

where of course energy conservation requires that $E = E_j + E_j^+ = E_{j'} + E_{j'}^+$. We have denoted by

$$\mathcal{C}_{qk}^{j'j} \equiv \hbar \sqrt{2\pi\hbar} \mathcal{Z}_{qk}^{j'j} \sqrt{2r_0 \sin \theta_{iq}} \quad (3.19)$$

the *diffraction coefficient*. C depends on the angles of the incoming and outgoing trajectories and on the quantum states of the core that determine the value of the T-matrix element $T_{j'j}$. We have used the fact that if $\mathbf{q}$ is in the outer region $S(0; \mathbf{q}) \simeq \sqrt{8r_0} + S(r_0, \theta; \mathbf{q})$ [14,27] to absorb the coefficient $e^{2i\sqrt{8r_0}}$ in the Green's function, which now formally propagates from the origin at $\mathbf{r} = 0$. Note that the diffraction coefficient also depends on r_0, which gives the internal scale of the inner zone diffraction. However, as is known from closed orbit theory for the photoabsorption cross section, we show below that the density of states does not depend on r_0. Finally, it may also be noted that G_D is of order $\sqrt{\hbar}$ relative to the "free" Green's function.

C. Diffractive density of states

1. Density of states

The fluctuation in the density of states (DOS)—formally proportional to $\text{Im}[\text{Tr}G]$—is obtained in the semiclassical limit by taking the trace of G_{sc} as [25]

$$d_0(E) = \frac{1}{2\pi\hbar} \sum_k A_k \exp iS_k + \text{c.c.} \quad (3.20)$$

with

$$A_k = \frac{\tau_k \exp - i(\mu_k + \sigma_k)\pi/2}{|\det(M_{(k)} - I)|^{1/2}}, \quad (3.21)$$

and where c.c. stands for complex conjugate and will be implicitly understood in the rest of the paper. We have as-

sumed the orbits are isolated; k runs on the periodic orbits and their repetitions and σ_k is an additional phase resulting from taking the trace. τ_k is the period and M the 2×2 stability matrix of the orbit with elements m_{np}. When diffractive effects are present, the total Green's function is given by the sum $G = G_0 + G_D$; the geometric DOS is given by Im[TrG_0], yielding Eq. (3.20), whereas the diffractive contribution to the DOS is obtained by taking the trace of G_D.

2. Taking the trace of G_D

To take the trace of Eq. (3.18), we first use the orthonormality of the states $|j\rangle$ and reduce the problem to two dimensions [24]. We can then set $j = j'$ and $k = q$, yielding

$$\text{Tr} G_D = \sum_j \sum_k \mathcal{C}_{kk}^{jj} \int dq\, dq^\perp G_{sc(k)}^j(\mathbf{r};0) G_{sc(k)}^j(0;\mathbf{r})$$

$$(3.22)$$

where $(q, q^\perp)$ are local coordinates along and perpendicular to the trajectory introduced in Sec. III B 1. Given the reduction from 3D to 2D, we choose for convenience $(q, q^\perp)$ so that relative to the cylindrical coordinates (ρ, z) the Jacobian is $\partial(\rho, z)/\partial(q, q^\perp) = (r \sin \theta)^{-1}$. The integral can now be performed, for each trajectory k, in the stationary phase approximation (a similar calculation is given in full detail by Bruus and Whelan [18]). To first order in $\hbar$, we obtain the approximate folding property for the semiclassical Green's function:

$$\text{Tr} G_D = \sum_j \sum_k \mathcal{C}_{kk}^{jj} \tau_k^j G_{sc(k)}^j(0;0)(i\hbar)^{-1}. \qquad (3.23)$$

The diffractive DOS is thus given in terms of the geometric ("free" hydrogenic) orbits k closed at the nucleus associated with every possible quantum state $|j\rangle$ of the scatterer, weighted by the diffraction coefficient C_{kk}^{jj}. As in closed orbit theory, the classical orbits k that hit the center of the core ($\mathbf{r} = \mathbf{0}$) are radial in the vicinity of the core: they leave the boundary circle with an initial angle θ_{ik} and return with a final angle θ_{fk}.

Equation (3.23) can be written (see Appendix B) in a form similar to the geometric DOS (3.20):

$$d_D(E) = \frac{1}{2\pi\hbar} \sum_j \sum_k \mathcal{A}_k^j \exp i S_k^j \qquad (3.24)$$

with

$$\mathcal{A}_k^j = \hbar^{1/2} e^{-i(\mu_k^j \pi/2 + 3\pi/4)} T_{jj} Y_{l_j m_j}$$

$$\times (\theta_{ik}) Y_{l_j m_j}^*(\theta_{fk}) \tau_k^j 2^{5/2} \pi^{3/2} \left| \frac{\sin \theta_{ik} \sin \theta_{fk}}{m_{12(k)}} \right|^{1/2};$$

$$(3.25)$$

m_{12} is an element of the stability matrix for the kth orbit, calculated by considering a deviation in momentum space perpendicular to the orbital motion. It may be noted that the diffractive contribution to the DOS is $\hbar^{1/2}$ suppressed relative to the geometric DOS and that it does not depend on r_0. As expected, $d_D(E)$ depends on the quantum properties of the scatterer (via the T matrix) and on the properties of the clas-

sical orbits of the scatterer-"free" system. This is a general characteristic that is found in other works based on the geometrical theory of diffraction. For completeness we point out that the formulas given above between Eqs. (3.10) and (3.25) need to be modified when k is the so-called parallel orbit ($\theta_{ik} = \theta_{fk} = 0$) [14,29]

IV. DIFFRACTIVE CONTRIBUTION TO THE SPECTRAL RIGIDITY

A. The spectral rigidity $\Delta(L)$

1. $\Delta(L)$ in terms of periodic orbits

The spectral rigidity $\Delta(L)$ is defined as the least-squares deviation of the staircase function from the best-fitting straight line over an energy range corresponding to L mean level spacings [28],

$$\Delta(L) \equiv \left\langle \min_{A,B} \frac{\langle d \rangle}{L} \int_{\varepsilon_0 - L/2\langle d \rangle}^{\varepsilon_0 + L/2\langle d \rangle} d\varepsilon [\mathcal{N}(\varepsilon) - A\varepsilon - B]^2 \right\rangle,$$

$$(4.1)$$

where $\langle d \rangle$ is the mean density and the outer angular bracket denotes an average over the starting points ε_0. $\mathcal{N}(E)$ is the spectral staircase function,

$$\mathcal{N}(E) = \int^E d\varepsilon\, d(\varepsilon). \qquad (4.2)$$

$\Delta(L)$ describes correlations between level sequences longer than the mean level spacing $\langle d \rangle^{-1}$, i.e., $L > 1$. Berry [1,30] showed that, provided the energy range $L/\langle d \rangle$ is classically small (though it may be semiclassically large), $\Delta(L)$ could be obtained in terms of periodic orbits as

$$\Delta(L) = \frac{1}{2\pi^2} \int_0^\infty \frac{d\nu}{\nu} \frac{K(\nu/\pi L)}{\nu/\pi L} G(\nu), \qquad (4.3)$$

where $\nu = L\tau/(2\hbar\langle d \rangle)$. The "orbit selection" function $G(\nu)$ is given in Appendix C. $K(\zeta)$ is the spectral form factor, defined as the Fourier transform of the two-point correlation function (with $\zeta = \tau/h\langle d \rangle$). In the semiclassical limit, $K(\zeta)$ is approximately given by [30]

$$K(\zeta) \simeq \frac{1}{2\pi\hbar\langle d \rangle} \left\langle \sum_{k,q} A_k A_q^* \exp[i(S_k - S_q)/\hbar] \delta\left(\tau - \frac{\tau_k + \tau_q}{2}\right) \right\rangle,$$

$$(4.4)$$

with the factors A_k given in Eq. (3.21).

Different approximations for $K(\zeta)$ have been discussed in [30]. They are appropriate for different values of ζ. Let ζ^* be such that $\tau_{\min}/h\langle d \rangle \ll \zeta^* \ll 1$ where $\tau_{\min}$ is the period of the shortest orbit. Then

$$K(\zeta) \approx \frac{1}{h\langle d \rangle} \sum_k |A_k|^2 \delta(\tau - \tau_k), \quad \zeta < \zeta^*, \qquad (4.5)$$

$$K(\zeta) \approx \zeta, \quad \zeta^* < \zeta < 1, \qquad (4.6)$$

$$K(\zeta) \approx 1, \quad \zeta > 1. \qquad (4.7)$$

Equation (4.5) is the diagonal approximation, which is valid for short periodic orbits and gives rise to nonuniversal (i.e., system-dependent) terms; in particular, the shortest orbit determines the spacing $L_{\max}$ for which the rigidity saturates (see Appendix C). Equation (4.6) is valid for long (but not too long) orbits and follows from a classical sum rule [31] in the diagonal approximation, which leaves no trace of any system-dependent dynamics; from Eq. (4.3), this form essentially contributes to the rigidity in the interval $1 \ll L \ll L_{\max}$. The form (4.7) is valid for long orbits beyond the Heisenberg time and is obtained by appealing to a semiclassical sum rule [1]; it contributes to $\Delta(L)$ for small values of L, but also contributes to rigidity through an additive constant term.

2. Geometric and diffractive contributions

Since the total fluctuations in the spectral DOS are given by $d(E) = d_0(E) + d_D(E)$, the same relation holds for the oscillating part of the spectral staircase function. It then follows from Eq. (4.1) that the spectral rigidity is obtained as the sum of three terms:

$$\Delta(L) = \Delta_{00}(L) + \Delta_{0D}(L) + \Delta_{DD}(L). \qquad (4.8)$$

$\Delta_{00}(L)$ is the rigidity for the "free" system: it involves only correlations between orbits of the free system, so that for $K_{00}(\zeta)$ the indices k and q in Eq. (4.4) refer to geometric periodic orbits. $\Delta_{0D}(L)$ involves correlations between geometric and diffractive orbits so that in the spectral form factor k and q refer, respectively, to geometric and diffractive orbits. In the same vein, $\Delta_{DD}(L)$ involves only correlations between diffractive orbits. In this work, we are interested only in the contribution $\Delta_{diff}(L)$ to the spectral rigidity provoked by the presence of the scatterer, which is the same as the difference between the spectral rigidity for the system and the rigidity for the scatterer-free system, since

$$\Delta_{diff}(L) \equiv \Delta(L;T) - \Delta_{00}(L) = \Delta_{0D}(L) + \Delta_{DD}(L); \quad (4.9)$$

we have explicitly written $\Delta(L;T) \equiv \Delta(L)$ to emphasize the the scatterer dependence through the T matrix.

B. Diffractive spectral rigidity for the scaled molecule

We now determine $\Delta_{diff}(L)$ for our model described in Secs. II and III. We first need the scaled equivalent of the formulas given above. We then use the following approximations. For $\Delta_{DD}(L)$ we employ the diagonal approximation for diffractive orbits. We obtain a classical sum in the isotropic approximation by relying on previous results obtained by Sieber [3]. For $\Delta_{0D}(L)$, we restrict the correlations to orbits having the same action and the same topology; this has the effect of taking into account the sole closed orbits at the

origin, but the amplitude factors entering $K_{0D}(\zeta)$ are different; we use a classical sum rule for off-diagonal contributions, adapted from the one that was obtained by Bogomolny et al. [4]. However, we cannot obtain a semiclassical sum rule without taking into account the correlation between geometric orbits that do not hit the origin and that make up $\Delta_{00}(L)$. Here, we restrict our attention to $\Delta_{diff}(L)$ and we will not therefore search for a semiclassical sum rule; as a result, the determination of $\Delta_{0D}(L)$ and $\Delta_{DD}(L)$ will hold only for $L \gg 1$. The constant term arising from the semiclassical sum rule is of no importance: in Sec V we compare the difference $\Delta(L;T) - \Delta_{00}(L)$ obtained from quantum mechanically calculated energy levels for systems with and without the scatterer. As argued in Sec. V A and Appendix D, the constant term can be taken to be the same in both systems, and therefore vanishes when the difference is taken.

1. Rigidity in scaled variables

The advantage of scaling the system is that the classical dynamics is invariant provided the scaled energy ϵ is fixed; the scaled amplitudes and actions $\tilde{A}(\epsilon)$ and $\tilde{S}(\epsilon)$ are then constant and the levels are obtained as a function of the parameter $\kappa \equiv \gamma^{-1/3}$. κ is varied in the interval $[\kappa_1, \kappa_2]$ and $\bar{\kappa}$ is the midpoint. The scaled action, defined by $\kappa \tilde{S}(\epsilon) \equiv S(E)/\hbar$, plays the role of both the action S and the period τ of the unscaled orbit, and κ plays the role of the energy and of $\hbar$; in the following, the notation $\hbar_{eff}$ stands for the mean value $\hbar_{eff} = \bar{\kappa}^{-1}$ of κ^{-1} in the interval $[\kappa_1, \kappa_2]$.

The oscillating part of the scaled DOS (at fixed ϵ) is

$$\tilde{d}(\kappa) = \frac{1}{2\pi} \sum_j \sum_k \tilde{A}_k^j \exp i\kappa \tilde{S}_k^j + \tilde{\mathcal{A}}_k^j \exp i\kappa \tilde{S}_k^j \quad (4.10)$$

with [cf. Eqs. (3.23) and (3.25)]

$$\tilde{A}_k = \frac{\tilde{S}_k \exp - i(\mu_k + \sigma_k)\pi/2}{|\det(\tilde{M}_{(k)} - I)|^{1/2}} \qquad (4.11)$$

and

$$\tilde{\mathcal{A}}_k^j = \hbar_{eff}^{1/2} \tilde{S}_k^j e^{-i(\mu_k^j \pi/2 + 3\pi/4)} T_{jj} Y_{l_j m_j}(\theta_{ik}) Y_{l_j m_j}^*$$

$$\times (\theta_{fk}) 2^{5/2} \pi^{3/2} \left| \frac{\sin \theta_{ik} \sin \theta_{fk}}{\tilde{m}_{12(k)}^j} \right|^{1/2}. \qquad (4.12)$$

It is straightforward to obtain the rigidity by following the original derivation leading from Eq. (4.1) to Eq. (4.3) [1] (actually, the derivation is simpler for scaled systems). Since the scaled spectra will be unfolded, we put $\langle \tilde{d} \rangle = 1$, and keep in mind that L scales as $\langle d \rangle$ previous to unfolding; the rigidity (4.3) is obtained by summing terms of the form

$$\Delta_{XY} = \frac{1}{2\pi^2} \int_0^\infty \frac{d\nu}{\nu} \frac{K_{XY}(\nu/\pi L)}{\nu/\pi L} G(\nu) \qquad (4.13)$$

with

$$\nu = \frac{LS}{2\chi}, \tag{4.14}$$

where $\chi \equiv \partial\langle N\rangle/\partial\kappa$. We will from now on omit the tildes from the scaled variables, as no confusion can arise. The index XY obviously refers to $X, Y = 0$ or D [cf. Eq. (4.8)]. The spectral form factor is now given by

$$K_{XY}(\sigma) \simeq \frac{1}{2\pi\chi}\left\langle \sum_{j,j'}\sum_{k,q} \{\mathbb{A}_{Xk}^j[\mathbb{A}_{Yq}^{j'}]^* \exp[i(S_k^j - S_q^{j'})\kappa_0]\}\delta \right.$$
$$\left. \times \left(S - \frac{S_k^j + S_q^{j'}}{2}\right)\right\rangle, \tag{4.15}$$

where $\mathbb{A}_{Xk}^j$ stands for A_k^j if $X=0$ and $\mathcal{A}_k^j$ if $X=D$; now we have $\sigma = S/2\pi\chi$. Here the angular brackets denote an average over the starting points κ_0.

2. Determination of Δ_{DD}

Strictly, the diagonal approximation would involve neglecting correlations whenever $S_k^j \neq S_q^{j'}$. We use the further approximation of neglecting correlations if $j \neq j'$: orbits belonging to different potential sheets are not correlated. For the small values of S that contribute to the nonuniversal part, this approximation holds except if accidentally two orbits belonging to different potential sheets have the same action. For larger actions, this approximation appears necessary if classical sum rules are to be used at all.

For short orbits ($\sigma < \sigma^*$ with $\sigma^* \ll 1$) the diagonal approximation simply gives terms of the form

$$\sum_j \sum_{k \in \{\sigma_k < \sigma^*\}} \frac{1}{2\pi^2}\left|\frac{\mathcal{A}_k^j(\epsilon_j)}{S_k^j(\epsilon_j)}\right|^2 G\left(\frac{LS_k^j(\epsilon_j)}{2\chi}\right). \tag{4.16}$$

For longer orbits, the classical sum rule needs to be evaluated independently for each quantum state $|j\rangle$ of the scatterer (since for each $|j\rangle$ we have an independent classical problem of an outer electron with scaled energy ϵ_j moving in the given diamagnetic potential sheet). We further assume an average initial and final angle $\bar{\theta} = \pi/4$. We now use the sum rule for transient orbits given in [3]; since the initial and final velocities are given by $\dot{r} = \sqrt{2/r}$ (in the inner zone), we have for each $|j\rangle$

$$\sum_k \left|\frac{1}{m_{12(k)}^j}\right|\delta(S - S_k^j) \approx \frac{2\pi}{\Sigma^j(\epsilon_j)}, \tag{4.17}$$

where $\Sigma^j(\epsilon_j)$ is the volume of the energy surface in the scaled phase space with scaled energy ϵ_j, which can be determined classically. The form factor then becomes

$$K_{DD}^j(\sigma > \sigma^*) \approx \frac{1}{2\pi\chi}\hbar_{eff}2^5\pi^4\sum_j \frac{1}{\Sigma^j}|T_{jj}|^2|Y_{l_jm_j}(\bar{\theta})|^4 S^2. \tag{4.18}$$

The rigidity Δ_{DD} is finally obtained by integrating the remaining term in Eq. (4.13),

$$\mathcal{I}(L) \equiv 2\pi\chi\int_{\sigma^*}^1 d\sigma G(\pi L\sigma), \tag{4.19}$$

which is given in the semiclassical limit by Eq. (C7).

3. Determination of Δ_{0D}

The short-orbit contribution to Δ_{0D} is similar to the short-orbit contribution to Δ_{DD}: as above we neglect correlations if $j \neq j'$ and, although the amplitudes of the geometric and diffractive orbits are different, the sum runs on the same orbits closed at the origin: we neglect correlations between diffractive orbits and geometric ones that are not closed at the origin. Hence, for $\sigma < \sigma^*$, we have

$$\sum_j \sum_{k \in \{\sigma_k < \sigma^*\}} \frac{1}{2\pi^2}\frac{1}{[S_k^j(\epsilon_j)]^2}A_k^j(\epsilon_j)[\mathcal{A}_k^j(\epsilon_j)]^* G\left(\frac{LS_k^j(\epsilon_j)}{2\chi}\right). \tag{4.20}$$

For longer orbits, we need the relevant classical sum rule. Starting from Eq. (4.15), with $X=0$, $Y=D$, and $j=j'$, we assume that K_{0D} has significant contributions from orbits with close actions, so that

$$S_k^j - S_q^j \approx -\frac{1}{2}W(\theta, \theta_i)\theta^2, \tag{4.21}$$

where W is the matrix of mixed second derivatives of $S(\mathbf{r}, \mathbf{r}')$. We also express the stability matrix element $1/m_{12(k)}^j$ taken on the boundary circle as

$$|m_{12(k)}^j|^{-1/2} = \left|\frac{\partial^2 S_k^j}{\partial\theta_i\partial\theta_f}\right|^{1/2}\sqrt{\frac{2}{r_0}} \tag{4.22}$$

and further remark that

$$|\det(M_{(k)}^j - I)|^{1/2}\left|\det\frac{\partial^2 S_k^j}{\partial\theta\partial\theta'}\right|^{1/2} = |\det W(\theta, \theta')|^{1/2}. \tag{4.23}$$

We can now use the generalized sum rule obtained in [4],

$$\sum_k \frac{\delta(S - S_k^j)\Omega^j(\mathbf{q}_k, \mathbf{p}_k)}{|\det(M_{(k)}^j - I)|} = \frac{1}{\Sigma^j}\int dq^\perp dp^\perp \Omega^j(\mathbf{q}, \mathbf{p}), \tag{4.24}$$

in which the DOS amplitude is multiplied by a "test function" $\Omega^j(\mathbf{q}_k, \mathbf{p}_k)$ defined on a surface of section that includes the scatterer and is orthogonal to the incoming trajectory. The obvious choice for Ω is to take the terms between braces in the sum (4.15) multiplied by $|\det(M_{(k)}^j - I)|$. Note that, since we have assumed that the trajectories are radial when they cross the boundary circle, the integration measure transverse to the motion of the orbit is reduced to $\sin\theta\sqrt{r_0/(4 + 4\cos\theta)}d\theta$. K_{0D} is then obtained by summing over the quantum states j the right-hand side of Eq. (4.24). We use again the average angle approximation $\bar{\theta} = \pi/4$, and Eqs. (4.21) and (4.23) then lead to a Gaussian integral. Hence

$$K_{0D}^j(\sigma > \sigma *) \approx \frac{-1}{2\pi\chi}\hbar_{eff}\frac{2^{9/2}\pi^3}{2\sqrt{2+\sqrt{2}}}\sum_j \frac{1}{\Sigma^j}i(T_{jj}-T_{jj}^*)$$

$$\times |Y_{l_j m_j}(\bar{\theta})|^2 S^2. \qquad (4.25)$$

Note that we took the average value $\bar{\kappa} \equiv \hbar_{eff}^{-1}$ for the starting points κ_0, so that the Gaussian integration brings about a factor $-\hbar_{eff}^{1/2}$ which multiplies the original factor $\hbar_{eff}^{1/2}$ in Eq. (4.20). The rigidity is obtained by performing the integral (4.19).

C. Results

We now summarize the theoretical results for the diffractive spectral rigidity obtained in the semiclassical limit. Collecting Eqs. (4.16), (4.18), (4.20), and (4.25) along with Eq. (4.13), we obtain

$$\Delta_{DD}(L) + \Delta_{0D}(L) = \sum_j \left\{ \sum_{k\in\{\sigma_k<\sigma*\}} \frac{1}{[\pi S_k^j]^2}(\mathrm{Re}[A_k^j \mathcal{A}_k^j] \right.$$

$$\left. + |\mathcal{A}_k^j|^2)G\left(\frac{LS_k^j}{2\chi}\right) \right\} + \sum_j \left[\frac{\hbar_{eff}|Y_{l_j m_j}(\bar{\theta})|^2}{\pi^2 \Sigma^j} \right.$$

$$\times \left(2^5 \pi^4 |T_{jj}|^2 |Y_{l_j m_j}(\bar{\theta})|^2 \right.$$

$$\left. \left. + \frac{2^{11/2}\pi^3}{3.7}\mathrm{Im}\, T_{jj} \right) \mathcal{I}(L) \right], \qquad (4.26)$$

where $\mathcal{I}(L)$ is given by Eq. (4.19). The term between the curly brackets represents a system-dependent nonuniversal contribution, which contains the shortest periodic orbits within each potential sheet $|j\rangle$ (from the shortest scaled action $S_{\min}^j$ up to some scaled action $S^{j*} \ll 2\pi\chi$). This term depends on the scatterer properties through the diffractive amplitude $\mathcal{A}_k^j$. The term between square brackets gives a contribution coming from averaging over orbits with scaled action $S^j \gg S_{\min}^j$ but shorter than the break time $2\pi\chi$. It is universal in the sense that it does not depend on the individual properties of the orbit, although since this is a diffractive contribution it obviously depends on the scatterer properties embodied in the T matrix. It may be noted that the nonuniversal term depends on $\hbar_{eff}$ (through $\mathcal{A}_k^j$), whereas the term between square brackets is independent of $\hbar_{eff}$: indeed $\mathcal{I}(L) \sim \chi$ [Eqs. (C6) and (C7)], and χ scales as $\hbar_{eff}^{-1}$, so that when $\hbar_{eff}$ is varied $\hbar_{eff}\chi$ is constant.

V. NUMERICAL RESULTS

A. Comparing quantum and semiclassical results

We give in this section numerical results obtained for our model by comparing the spectral rigidity obtained from a calculation of exact quantum eigenvalues to our semiclassical approximation as given by Eq. (4.26). More specifically, as stated in Sec. IV A 2, we are interested only in the *diffractive* contribution to the spectral rigidity. Quantum mechanically, this involves performing calculations for the scatterer-free system on the one hand [we obtain the rigidity $\Delta_{00}(L)$;

cf. Eq. (4.8)], and for the system with the scatterer on the other hand [we then obtain the rigidity $\Delta(L;T) \equiv \Delta(L)$; cf. Eq. (4.9)]. The quantum mechanical determination of the diffractive contribution to the spectral rigidity is therefore given by calculating the difference $\Delta(L;T) - \Delta_{00}(L)$. Following Eq. (4.9), this difference should be equal in the semiclassical limit to the sum $\Delta_{0D}(L) + \Delta_{DD}(L)$. However, as mentioned in Sec. IV A, the semiclassical expression for the rigidity involves the contributions of orbits with periods beyond the Heisenberg time, which are taken into account through the relevant expression of the form factor obtained from a semiclassical sum rule due to Berry [1]. According to the semiclassical sum rule, those long orbits generate the mean level density. Based on the numerical evidence that the systems with and without the scatterer have approximately the same mean density, we assume that long orbits do not contribute to the diffractive part of the spectral rigidity; this heuristic argument is developed in Appendix D. The upshot is that we can compare the quantity $\Delta(L;T) - \Delta_{00}(L)$ obtained from accurate quantum mechanical calculations to the semiclassical expression (4.26) provided we are interested in correlations in the range $L \gg 1$.

B. Results

1. Calculations

We calculated a set of eigenvalues for a scaled molecule in the symmetry state $M = 0$, with a rotational constant chosen so that the scaled energies are $\epsilon_{N=0} = -0.55$ and $\epsilon_{N=2} = -0.8$, in the range $\kappa = 80$ to $\kappa = 150$, with average $\hbar_{eff} \simeq 0.01$. Such calculations involve about 10 000 states. The computational method was described elsewhere [14]. $\chi \simeq 148.8$ is readily calculated by fitting the spectral staircase to a second order polynomial in κ. Classical calculations for the shortest orbits are necessary to determine the nonuniversal contribution; these include the actions, monodromy matrix elements, and Maslov indices of the orbits closed at the nucleus in the scaled hydrogenic problem at the relevant scaled energies. Σ is determined for the relevant values of the scaled energies from the surface of the energy shell in configuration space.

2. Results

Quantum results for the spectral rigidity are plotted in Fig. 2 for different values of the quantum defects, i.e., for systems with cores having different properties. Indeed, it follows from Eqs. (2.2) and (2.3) and from the unitarity of the frame transformation that if $\mu_\Sigma = \mu_\Pi$ the T matrix is diagonal in the scatterer quantum numbers N, M_N: from a physical standpoint, this means there is only *elastic* scattering, i.e., the electron stays within the same potential sheet when it scatters off the core. When $\mu_\Sigma \neq \mu_\Pi$, the T matrix is not diagonal and mixings between Rydberg series belonging to the $N=0$ core state on the one hand and the $N=2$ $(M_N=-1,0,1)$ core state on the other occur; physically, this means both elastic and inelastic scattering occur, the relative strength between them being determined by the T-matrix elements $T_{jj'}$.

Figure 2 shows the value of the spectral rigidity determined from quantum mechanical calculations. Figure 2(a)
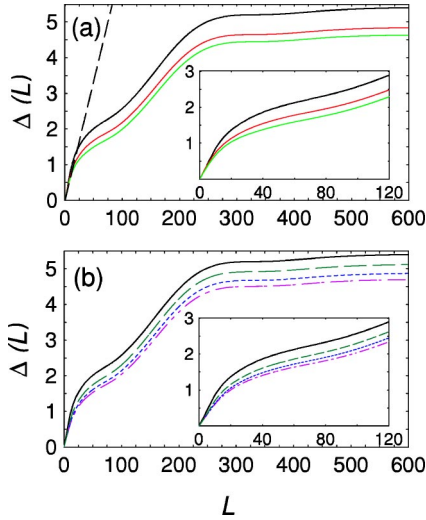
FIG. 2. Spectral rigidity determined from calculated quantum spectra. (a) The black solid curve corresponds to the scatterer-free system whereas the curves underneath correspond to two examples of systems with equal quantum defects allowing only for elastic scattering: $\mu_\Sigma=\mu_\Pi=-0.25$ (upper line) and below $\mu_\Sigma=\mu_\Pi=0.5$ (lower line). The straight dashed line is the $L/15$ limiting curve. (b) The black solid curve corresponds again to the scatterer-free system and the curves underneath to systems with scatterers allowing for inelastic scattering: from top to bottom $\mu_\Sigma=0.22\ \mu_\Pi=-0.06$ (dashed curve), $\mu_\Sigma=0.5\ \mu_\Pi=0$ (dotted line), and $\mu_\Sigma=0.5\ \mu_\Pi=-0.15$ (dot-dashed curve). In each case, the inset gives an enlarged view of the rigidity for small L.

shows the rigidity $\Delta_{00}(L)$ for the scatterer-free system (black solid line) as well as two examples of a scatterer allowing only elastic scattering ($\mu_\Sigma=\mu_\Pi=0.5$ and $\mu_\Sigma=\mu_\Pi=-0.25$). Figure 2(b) again shows $\Delta_{00}(L)$ as well as three cases of systems with a core allowing also for inelastic scattering ($\mu_\Sigma=0.5\ \mu_\Pi=0,\mu_\Sigma=0.5,\mu_\Pi=-0.15$, and the H_2 molecule case with quantum defects $\mu_\Sigma=0.22,\mu_\Pi=-0.06$). The generic shape of these curves shows an inflection around $L\sim50$ and saturation starting at $L\sim275$. This is semiclassically related to the saturation of the orbit selection function for each dynamical regime.

Figure 3(a) shows the difference $\Delta(L,T)-\Delta_{00}(L)$ for quantum calculations, which we defined above as the diffractive contribution to the spectral rigidity. Figure 3(b) displays our semiclassical results, obtained by appying Eq. (4.26). For each dynamical regime ($\epsilon_{N=0}=-0.55$ and $\epsilon_{N=2}=-0.8$), we included about a dozen orbits, so that in the corresponding hydrogenic cases $\sigma^*\simeq0.1$. The main features of the quantum results are well reproduced by our semiclassical calculations: in particular, the first inflection at $L\sim50$ and the saturation at $L\sim275$ are clearly reproduced. The first inflection is due to the saturation of the orbits associated with the scatterer in the $N=0$ state. Application of Eq. (C3) for the dynamics at $\epsilon_{N=0}=-0.55$ would, however, yield a larger value of $L_{max}^{N=0}$ than is observed in both the quantum and the semiclassical calculations. The reason is that the shortest orbit (perpendicular to the field) has small geometric and diffractive amplitudes compared to the large amplitudes of the longer balloon orbit (which lies in scaled energy just above
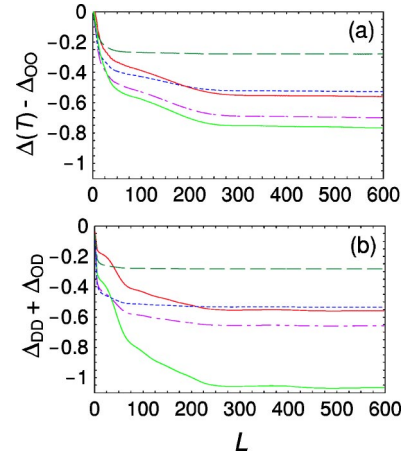
FIG. 3. Diffractive contribution to the spectral rigidity for systems with different scatterers whose properties depend on the values of the quantum defects: going from the most rigid to the less rigid spectrum we have $\mu_\Sigma=0.22\ \mu_\Pi=-0.06$ (dashed curve), $\mu_\Sigma=0.5\ \mu_\Pi=0$ (dotted curve), $\mu_\Sigma=\mu_\Pi=-0.25$ (upper solid line), $\mu_\Sigma=0.5\ \mu_\Pi=-0.15$ (dot-dashed curve), and $\mu_\Sigma=\mu_\Pi=0.5$ (lower solid line). (a) shows the results obtained from quantum calculations by subtracting the curves for systems with scatterers in Fig. 2 from the scatterer-free system line. (b) displays the semiclassical results obtained within the approximations discussed in the text.

its bifurcation point from the orbit parallel to the field). The saturation of the diffractive rigidity visible beyond $L\sim275$ corresponds to the shortest orbit existing in the $N=2,\ |M|=1$ potential sheets; the contribution of the orbits in the $N=2,\ M=0$ potential sheet is considerably less important, due to the fact that the orbit perpendicular to the field (the main orbit at $\epsilon=-0.8$) is suppressed in the diffractive process when $m=0$ [32]. Note that in the case $\mu_\Sigma=0.22\ \mu_\Pi=-0.06$ the curve saturates at $L\sim50$ rather than displaying an inflection: this is readily explained by the fact that, for such values of the quantum defects, the T-matrix elements $T_{2\pm1,2\pm1}$ are very small and therefore the contribution of the $N=2,\ |M|=1$ potential sheets to the diffractive rigidity is negligible; the orbits associated with the scatterer in the $N=0$ state dominate the shape of the curve, and the second saturation at $L\sim275$ is hardly visible. Generally speaking, the slopes of the curves in the three main intervals ($L<50,50<L<275,$ and saturation for $L>275$) depend on the strength of the T-matrix elements. They also depend on the relative strengths of the universal and nonuniversal terms. In particular, note the crossing at $L\sim200$ between the curves corresponding to scatterers having $\mu_\Sigma=0.5\ \mu_\Pi=0$ and $\mu_\Sigma=\mu_\Pi=-0.25$, which is adequately reproduced by the semiclassical calculations. This crossing results from the competition between the nonuniversal and universal terms; the nonuniversal terms (which dominate the curve for large L) are larger in the $\mu_\Sigma=\mu_\Pi=-0.25$ case, whereas the universal terms are considerably larger for a core scatterer with $\mu_\Sigma=0.5\ \mu_\Pi=0$.

C. Discussion

We have seen that the semiclassical formalism developed above gives an adequate explanation of the diffractive rigid-

ity obtained from the quantum mechanical levels. We now discuss further aspects, and in particular the limitations of the results presented in this paper.

The main limitation, not yet mentioned, concerns the sensitivity of Eq. (4.26) to the number of orbits included in the nonuniversal part of $\Delta_{GD}+\Delta_{DD}$. As more orbits are added, the curves for the diffractive rigidity tend to be translated (generally downward). In his discussion of this tiny but important range composed of nonuniversal terms, Berry [30] pointed out that the final result would be independent of the number of orbits included in the nonuniversal part, provided the condition $\zeta<\zeta^*$ was respected [see Eq. (4.5)]. This was not the case here, and although the shapes of the different curves were not modified when the number of orbits included in the nonuniversal part was increased, the value of $\Delta_{GD}+\Delta_{DD}$ on the vertical scale changed, since the curves underwent an overall translation. To plot Fig. 3(b), we have accordingly rescaled the semiclassical results so that the saturation value concords approximately with the quantum results. We emphasize that all the semiclassical results were multiplied by an identical global factor (so that the rescaling is related only to the number of orbits in the nonuniversal term independently of the scatterer properties). The reason for such a behavior may be related to the fact that our scaled energies correspond to a phase space of mixed type: instead of having amplitudes exponentially decreasing with the period (as would be expected in a chaotic regime), our classical calculations display strong focusing effects, yielding large amplitudes for certain orbits or their repetitions, independently of their length (this is of course typical of stable orbits in mixed phase space). Moreover, we have employed classical sum rules generally valid for a chaotic phase space in a mixed phase space situation. Indeed, the ergodic average, if properly done, should not be taken on the entire energy surface, since a fraction of the orbits are confined to invariant tori (but then it is not obvious, given the approximations made, how to derive mean properties of a typical orbit). Of course, the derivation of the diffractive Green's function is valid regardless of whether the classical motion is chaotic or not, provided the diffractive orbits are isolated. We also note at this point that exploring the chaotic regime (which would be more meaningful for comparing quantum and semiclassical results from a quantitative standpoint) would involve quantum calculations at higher scaled energies, and therefore higher energies if κ is kept constant, which would be computationally too expensive.

Another limitation is visible by observing the curve for $\mu_{\Sigma}=\mu_{\Pi}=0.5$, which is relatively larger in the semiclassical calculations than the quantum results indicate. The most probable cause for this mismatch is due to the inclusion of a single scattering in the formulas derived in this paper. Indeed, although each scattering process is reduced by a factor $\hbar^{1/2}$ [cf. Eq. (3.25)], for finite values of $\hbar$ diffractive orbits with more than one core scatterer will need to be included if the T matrix is large or m_{12} is very small for the orbits included in the nonuniversal term. For $\mu_{\Sigma}=\mu_{\Pi}=0.5$ the diagonal T-matrix elements are maximally large, and for $\epsilon=-0.55$ many of the shortest orbits have a large classical amplitude (small m_{12}). Therefore diffractive orbits with multiple core scatterers will probably have a more important
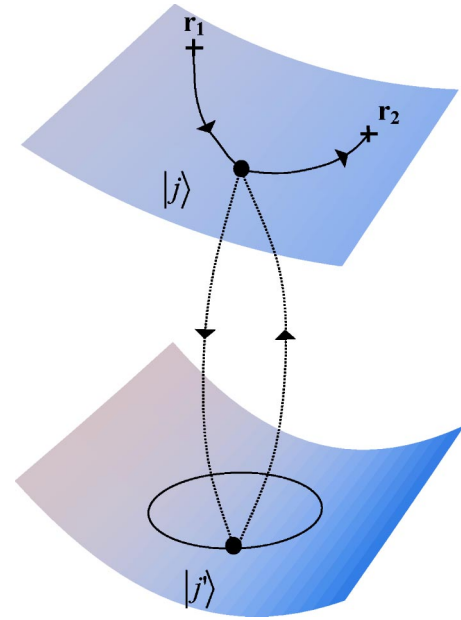
FIG. 4. Example of a higher-order process with multiple scattering: a wave travels from $\mathbf{r}_1$ to $\mathbf{r}_2$ in the same potential sheet after scattering twice with the core and having followed a closed orbit in another potential sheet.

effect than for smaller values of the T matrix. Note that such orbits can involve combinations of closed loops belonging to different potential sheets (i.e., built on different core states), as portrayed on Fig. 4. On the other hand, due to the scaling properties of our problem (in particular, the scaled phase space volume does not depend on $\hbar$), we do not expect a significant contribution from the mean properties of long orbits with multiple core scatterers, obtained by successive application of the classical sum rules [3].

It was recently shown that in chaotic systems with a pointlike interaction (a δ scatterer), the off-diagonal contributions to the form factor (diagonal or geometric correlations encapsulated here in K_{0D}) canceled exactly the contribution arising from correlations between diffractive orbits (encapsulated in K_{DD}-like terms) [4,5]. The underlying reason for this effect, due to the conservation of the probability during the scattering process, is based on the unitarity relations for the (single channel) T-matrix element. It is therefore of interest to see whether such a cancellation occurs in the present case. In the multichannel case, the unitarity equation for the diagonal elements reads [33]

$$\text{Im}\, T_{jj} + \sum_i |T_{ji}|^2 = 0. \tag{5.1}$$

Therefore, comparing with Eq. (4.26), we see that in the general case, to lowest order in $\hbar$, there is no cancellation between the geometric or diffractive correlations and the "diagonal" diffractive correlations because of the nondiagonal T-matrix elements, and this is indeed verified in our calculations. Comparing Eq. (5.1) with Eq. (4.26), we see, however, that the universal term inside the square brackets in Eq. (4.26) approximately vanishes if the T matrix is diagonal and $m=0$. We noted above that when $\mu_{\Sigma}=\mu_{\Pi}$ the nondiagonal

T-matrix elements do vanish, but the universal terms in Eq. (4.26) are not simultaneously canceled for all the values of *j*. This feature appears as a consequence of the approximations made in deriving Eqs. (4.18) and (4.25) rather than a generic characteristic of multilevel scatterers.

VI. CONCLUSION

In this work, we have derived the corrections to the density of states when a multilevel scatterer is added to a system that can be treated semiclassically. We employed as a model a scaled Rydberg molecule in a magnetic field. The core–Rydberg-electron collision results in a "diffraction" of the semiclassical waves, accompanied by a change in the potential sheet of the outer electron. The relevant Green's function was obtained and employed to derive a first-order semiclassical expression giving the diffractive contribution to the spectral rigidity. This expression was tested by comparing with the spectral rigidity obtained from accurate quantum calculations, yielding a qualitative and semiquantitative agreement. Indeed, semiclassics gives an interpretation of the spectral statistics that cannot be obtained in any other way. The quantitative results, while reproducing the main features of the diffractive contributions to the rigidity, suffer from the shortcomings discussed above. It does appear, however, that these shortcomings arise from system specifics (mixed phase space, $\hbar$ not small enough) rather than hinging on the method employed.

APPENDIX A

We relate the propagation of the density as it appears in Eq. (3.13) to the prefactor in the semiclassical Green's function by directly evaluating

$$J(t,q_0^\perp) = \left.\frac{\partial q}{\partial t}\right|_{q_0^\perp} \left.\frac{\partial q}{\partial q_0^\perp}\right|_t - \left.\frac{\partial q^\perp}{\partial t}\right|_{q_0^\perp} \left.\frac{\partial q}{\partial q_0^\perp}\right|_t \quad (A1)$$

for our problem at hand. The index 0 refers to the initial point, which is located on the initial surface (the boundary circle). We assume $q_0^\perp$ is a cyclic coordinate, and since $\dot{q}^\perp \equiv 0$ we obtain by manipulating partial derivatives that

$$\left.\frac{\partial q^\perp}{\partial t}\right|_{q_0^\perp} = 0 \quad (A2)$$

and

$$\left.\frac{\partial q^\perp}{\partial p_0^\perp}\right|_{q_0^\perp} = \left.\frac{\partial q^\perp}{\partial p_0^\perp}\right|_t. \quad (A3)$$

We now use $\partial q/\partial t|_{q_0^\perp} = \dot{q}$ and the above equation to establish

$$J(t,q_0^\perp)^{-1} = \frac{1}{\dot{q}} \left.\frac{\partial p_0^\perp}{\partial q^\perp}\right|_{q_0^\perp} \left.\frac{\partial q_0^\perp}{\partial p_0^\perp}\right|_t \quad (A4)$$

$$= D\dot{q}_0 \left.\frac{\partial q_0^\perp}{\partial p_0^\perp}\right|_t. \quad (A5)$$

The last term in Eq. (A5) is evaluated explicitly on the boundary circle (where the magnetic field is negligible and

the Hamiltonian just incorporates the Coulomb field).

For example, if we use polar coordinates, the initial Jacobian on the boundary $J_3(t_0, \theta_{iq})$ that appears in Eqs. (3.13) and (3.15) becomes

$$J_3(t_0, \theta_{iq}) = r_0^2 \sin \theta_{iq} \dot{r} \quad (A6)$$

where we put

$$\left.\frac{\partial \theta_{iq}}{\partial p_{\theta_{iq}}}\right|_t = \dot{r}|_{r=r_0} = (r_0/2)^{-1/2} \quad (A7)$$

since we assume $p_{\theta_{iq}} = 0$ on the boundary circle. If we use another set of coordinates $(q, q^\perp)$ as in Sec. III C 2, then

$$\dot{q} = \frac{\partial(q, q^\perp)}{\partial(r, \theta)} \dot{r}. \quad (A8)$$

APPENDIX B

To obtain the amplitude term of the diffractive DOS as given in Eq. (3.25), it is useful to start from the Green's function between points on the boundary surface $G_{sc(k)}^j(r_0, \theta_{ik}; r_f, \theta_{fk})$. Using the coordinate system given in Sec. III C 2 and transforming back to polar coordinates, we have, using Eqs. (A7) and (A8),

$$G_{sc(k)}^j(\mathbf{r}_i; \mathbf{r}_f) = \frac{1}{\hbar\sqrt{2\pi\hbar}} \frac{1}{r_0^{5/4} 2^{3/4} \sqrt{\sin\theta_{ik}\sin\theta_{fk}}} \left|\frac{\partial\theta_{ik}}{\partial\theta_{fk}}\right|^{1/2}$$
$$\times \exp\{i[S_k(\mathbf{r}', \mathbf{r}) - \mu_k\pi/2 - 3\pi/4]\}. \quad (B1)$$

Equation (3.25) is obtained by expressing the angular derivative in terms of the stability matrix element $m_{12(k)}$ expressed in semiparabolic coordinates (see, e.g., [27]) as

$$\left|\frac{\partial\theta_{ik}}{\partial\theta_{fk}}\right| = \frac{r_0^{1/2}}{2^{1/2}m_{12(k)}}. \quad (B2)$$

APPENDIX C

Whereas the spectral form factor contains information specific to geometric or diffractive orbits, the shape of the spectral rigidity depends on the orbit selection function

$$G(\nu) \equiv 1 - F^2(\nu) - 3[F'(\nu)]^2, \quad (C1)$$

where $F(\nu) = \sin\nu/\nu$. Following the scaling properties, we have

$$\nu = \frac{LS^j}{2\chi} = \pi L\sigma^j. \quad (C2)$$

The orbit selection function saturates when the argument $\nu \gtrsim \pi$. The maximum value of L at which $G(\nu)$ saturates is therefore given by

$$L_{max}^j = \frac{2\pi\chi}{S_{min}^j}, \quad (C3)$$

where S_{min}^j is the scaled action of the shortest classical orbit in the potential sheet corresponding to the scatterer in state

$|j\rangle$. We will drop the index j below, but we emphasize that since the particle in our system can be in different potential sheets, there are different values of L_{max}. We therefore expect inflections in the shape of the spectral rigidity when the accumulation of orbits in the potential sheet $|j\rangle$ reaches the shortest orbit. The saturation observed in the rigidity corresponds to the potential sheet with the shortest orbits: here the scaled action of the shortest orbit decreases with the scaled energy.

Whereas in the scatterer-free system the rigidity involves (in the range $1 \ll L \ll L_{max}$ for which the classical sum rule form of the form factor is appropriate) integrals of the form

$$\int_{\sigma*}^{1} \frac{d\sigma}{\sigma} G(\pi L \sigma), \tag{C4}$$

the relevant integral for the diffractive contributions to the spectral rigidity is

$$\mathcal{J}(L) = \int_{\sigma*}^{1} d\sigma G(\pi L \sigma)$$

$$= \frac{1}{2\pi^4 L^4 y^3} [-1 - 2\pi^2 L^2 y^2 (2 + \pi^2 L y + \pi^2 L^2 y^2)$$

$$+ (1 + 2\pi^2 L^2 y^2) \cos 2L\pi y + 2\pi L y \sin 2L\pi y$$

$$+ 4\pi^3 L^3 y^3 \text{Si} 2L\pi y]|_{y=1}^{y=\sigma*}. \tag{C5}$$

(Si stands for sine integral.) Note that, for large values of $L \gg L_{max}$, $\mathcal{J}(L) \approx 1$ and therefore the integral $\mathcal{I}(L)$ defined by Eq. (4.19) as $\mathcal{I}(L) = 2\pi \chi \mathcal{J}(L)$ behaves as

$$\mathcal{I}(L \gg L_{max}) \approx 2\pi \chi. \tag{C6}$$

For general values of L, it is furthermore easy to show that in the semiclassical limit $\hbar_{eff} \to 0$, we have

$$\mathcal{I}(L) \approx \frac{\chi}{\pi^3 L^4}[1 + 4\pi^2 L^2 + 2\pi^4 L^4 - (1 + 2\pi^2 L^2)\cos 2\pi L$$

$$- 2\pi L \sin 2\pi L - 4\pi^3 L^3 \text{Si} 2\pi L]. \tag{C7}$$

APPENDIX D

Employing the index D as a shorthand for the overall diffractive contributions (i.e., $\Delta_D \equiv \Delta_{0D} + \Delta_{DD}$), we have $\Delta(L) = \Delta_0(L) + \Delta_D(L)$. Each of these two terms is written in terms of the form factor with the help of Eq. (4.13). It then follows that

$$\Delta(L) - \Delta_0(L) = \left[\Delta_D(\sigma < \sigma*) + \frac{\chi}{\pi} \int_{S*}^{2\pi\chi} K_D(\sigma) G(\nu) \frac{dS}{S^2} \right]$$

$$+ \mathcal{E}. \tag{D1}$$

The term between square brackets is our semiclassical result (4.26). Using $G(\nu) \sim 1$ for long orbits (and $L \gg 1$), $\mathcal{E}$ can be formally written as

$$\mathcal{E} = \frac{\chi}{\pi} \int_{2\pi\chi}^{\infty} [K_0(\sigma) + K_D(\sigma)] \frac{dS}{S^2} - \frac{\chi}{\pi} \int_{2\pi\chi}^{\infty} [K_0(\sigma)] \frac{dS}{S^2}. \tag{D2}$$

But since with a suitable limiting process the Laplace transform of the form factor yields the mean level density, the fact that the mean level densities are the same in systems with and without a scatterer indicates that $\mathcal{E} \sim 0$. Note that this is consistent with the $L/15$ behavior observed for small L in Fig. 2, which is independent of the core properties. To this approximation, Eq. (D1) indicates that our semiclassical result (4.26) is identical with the difference $\Delta(L) - \Delta_0(L)$ that we calculate quantum-mechanically.

[1] M. V. Berry, Proc. R. Soc. London, Ser. A **400**, 229 (1985).
[2] G. Vattay, A. Wirzba, and P. E. Rosenqvist, Phys. Rev. Lett. **73**, 2304 (1994).
[3] M. Sieber, J. Phys. A **32**, 7679 (1999).
[4] E. Bogomolny, P. Leboeuf, and C. Schmit, Phys. Rev. Lett. **85**, 2486 (2000).
[5] M. Sieber, J. Phys. A **33**, 6263 (2000).
[6] S. Rahav and S. Fishman, Nonlinearity **15**, 1541 (2002).
[7] E. Bogomolny and O. Giraud, Nonlinearity **15**, 993 (2002).
[8] A. Hönig and D. Wintgen, Phys. Rev. A **39**, 5642 (1989).
[9] P. N. Walker and T. S. Monteiro, Phys. Rev. E **61**, 6444 (2000).
[10] M. Lombardi and T. H. Seligman, Phys. Rev. A **47**, 3571 (1993).
[11] H. Friedrich and D. Wintgen, Phys. Rep. **183**, 37 (1989).
[12] P. A. Dando, T. S. Monteiro, D. Delande, and K. T. Taylor, Phys. Rev. A **54**, 127 (1996).
[13] A. Matzkin and T. S. Monteiro, Phys. Rev. Lett. **87**, 143002 (2001).
[14] A. Matzkin, P. A. Dando, and T. S. Monteiro, Phys. Rev. A **66**, 013410 (2002).

[15] X. H. He, K. T. Taylor, and T. S. Monteiro, J. Phys. B **28**, 2621 (1996).
[16] H. M. Nussenzveig, *Diffraction Effects in Semiclassical Scattering* (Cambridge University Press, Cambridge, England, 1992); J. B. Keller, J. Opt. Soc. Am. **52**, 116 (1962).
[17] N. Pavloff and C. Schmit, Phys. Rev. Lett. **75**, 61 (1995); H. Primack, H. Schanz, U. Smilansky, and I. Ussishkin, *ibid.* **76**, 1615 (1996); E. Bogomolny, N. Pavloff, and C. Schmit, Phys. Rev. E **61**, 3689 (2000).
[18] H. Bruus and N. D. Whelan, Nonlinearity **9**, 1023 (1996).
[19] P. A. Dando, T. S. Monteiro, and S. M. Owen, Phys. Rev. Lett. **80**, 2797 (1998).
[20] M. L. Du and J. B. Delos, Phys. Rev. A **38**, 1913 (1988).
[21] M. C. Gutzwiller, *Chaos in Classical and Quantum Mechanics* (Springer, Berlin, 1990).
[22] V. P. Maslov and M. V. Fedoriuk, *Semi-Classical Approximation in Quantum Mechanics* (Reidel, Dordrecht, 1981); see also J. B. Delos, Adv. Chem. Phys. **65**, 161 (1986) for a simplified presentation.
[23] R. G. Littlejohn, J. Stat. Phys. **68**, 7 (1992).
[24] S. Pal and D. Biswas, Phys. Rev. E **57**, 1475 (1998).

[25] M. Brack and R. Bhaduri, *Semiclassical Physics* (Addison-Wesley, Reading, MA, 1997).

[26] A. Matzkin, Phys. Rev. A **59**, 2043 (1999).

[27] B. Hüpper, J. Main, and G. Wunner, Phys. Rev. A **53**, 744 (1996).

[28] T. Guhr, A. Müller-Groeling, and H. A. Weidenmuller, Phys. Rep. **299**, 189 (1998).

[29] J. Gao and J. B. Delos, Phys. Rev. A **46**, 1455 (1992).

[30] M. V. Berry, in *Chaos et Physique Quantique*, edited by M.-J. Giannoni, A. Voros, and J. Zinn-Justin (Elsevier, Amsterdam, 1991), p. 251.

[31] J. H. Hannay and A. M. Ozorio de Almeida, J. Phys. A **17**, 3429 (1984).

[32] A. Matzkin, P. A. Dando, and T. S. Monteiro, Phys. Rev. A **67**, 023402 (2003).

[33] C. J. Joachain, *Quantum Collision Theory* (Elsevier, Amsterdam, 1975).